Available online at www.sciencedirect.com
SCIENCE DIRECT®
Pergamon
Cement and Concrete Research 34 (2004) 941–947
CEMENT AND CONCRETE RESEARCH

High-alumina cement production from FeNi-ERF slag, limestone and diasporic bauxite

E. Dourdounis[a], V. Stivanakis[a], G.N. Angelopoulos[a], E. Chaniotakis[b], E. Frogoudakis[c], D. Papanastasiou[d], D.C. Papamantellos[a,*]

[a] *Laboratory of Metallurgy, Chemical Engineering Department, School of Engineering, University of Patras, Karatheodori 1, 26500 Patras, Greece*
[b] *Department of Research and Development, Titan Cement Company SA, Kamari Plant Viotias, P.O. Box, 19200 Elefsis, Greece*
[c] *GMMSA LARCO, Amalias 20 and Souri 5, 10557, Athens, Greece*
[d] *Silver and Baryte Ores Mining Co. S.A., 21A Amerikis Street, 106 72, Athens, Greece*

Received 6 December 2001; accepted 2 November 2003

Abstract

In this paper the utilization of ferronickel electroreduction furnace (FeNi-ERF) slag for the production of high-alumina cement (HAC) is investigated through laboratory and pilot-scale tests. The process followed consisted of smelting reduction of slag mixtures with low-grade diasporic bauxite and limestone. In the laboratory-scale trials the main process parameters were defined, concerning raw material proportions, kinetics of the reductions and cooling rate of the product. The presence of a carbon-containing iron bath enhances FeO_x reduction from the slag. Products from laboratory tests developed satisfactory compressive strengths relative to those of commercial HAC. According to the results of the laboratory tests, pilot-scale heat treatments were carried out in a 5-t electric arc furnace (EAF) and about 4 t of final mixture were produced.

Keywords: ERF slag; Waste management; Cement manufacture; Calcium aluminate cement

1. Introduction

Ferronickel (FeNi; 100 kt/y, Ni 20% wt) and alumina/aluminium (750 and 160 kt/y, respectively) are among the main industrial products of Greece. The production of FeNi leads to "metallurgical wastes" at LARCO in Larymna of about 2000 kt/y of ERF slag, 180 kt/y rotary kiln gas-cleaning-system dust and 120 kt/y converter slag. Aluminium production, on the other hand, is related with the production of about 600 kt/y red mud and other by-products from bauxite beneficiation prior to its refining into alumina.

The most important contribution in the recycling of these wastes is made by the local cement industries, which are using about 25% of the above-mentioned slags in the production of Portland cement. However, increased industrial production during the last few years and at the same time the implementation of new environmental legislation forces the respective metallurgical industries to find either new applications or better disposal solutions for their generated residues other than depositing them in the North Euboian and Corinthian Bay.

Two principal methods are used today for the manufacture of high-alumina cement (HAC); one is sintering, as in the case of Portland cement manufacture, and the other, most widespread method, is fusion. The latter may be subdivided into [1,2] the following:

(1) *Continuous fusion method*, originally, the blast furnace/cupola process (with replacement of iron burden/scrap with bauxite in the raw feed but in the presence of coke, i.e., under reducing conditions) and, mainly today, the L-type furnace or Lafarge process [2,3] (with proportional amounts of bauxite and limestone charged into the vertical part and fuel injected in the horizontal one, i.e., under oxidizing conditions).
(2) *Batch smelting method*, using electric arc furnaces (EAFs), as in the case of ferroalloy production.

In this paper, a new process for the production of HAC from FeNi-ERF slag, low-grade diasporic bauxite

* Corresponding author. Fax: +30-61-990917.
E-mail address: pap@chemeng.upatras.gr (D.C. Papamantellos).

0008-8846/$ – see front matter © 2004 Elsevier Ltd. All rights reserved.
doi:10.1016/j.cemconres.2003.11.004

Table 1
Chemical analysis (wt.%) of LARCO's ERF slag used in the tests

SiO_2	CaO	Al_2O_3	Cr_2O_3	NiO	Fe_2O_3	FeO	MgO	LOI
34.31	14.12	5.73	3.50	0.26	10.33	37.55	1.97	0.00

LOI, loss on ignition.

and limestone as raw materials is presented. The main differences of this process in comparison with the usual methods mentioned above are the smelting reduction conditions of the process and, especially, the use in the furnace raw feed of low-cost industrial residues and products from metallurgical and mining operations. Besides the FeNi slag, low-grade diasporic bauxite replaces the expensive white-calcined bauxite used in the production of HAC in the L type. Furthermore, the proposed reduction smelting process allows for the recovery of the nickel and iron values contained in the molten ERF slag and also in the bauxite.

During the last two decades, extensive work has been carried out by the Laboratory of Metallurgy (METLAB) of the University of Patras to find new ways of maximizing the recycling percentage of several industrial residues. As a result of these extended efforts, the utilization since 1981 of 300 to 600 kt/y fly ash from the Megalopolis acid lignite power plant as a pozzolanic material in Portland cement production [4,5] should be mentioned.

2. Chemical analysis and mineralogical constituents of HAC cements

HACs are considerably more expensive than Portland cements (around four to five times as expensive) and so do not compete with the latter in any application where conventional or high-performance concrete made with Portland cement performs satisfactorily. However, there are applications in which the unique properties of HACs enable them to be used in severe environments. Such high-performance concretes extend the range of applications for cementitious materials.

The main oxides present in commercial HAC are CaO and Al_2O_3 at nearly equal amounts (30–42% and 35–50%, respectively). These oxides combine to form calcium aluminates (mainly CA and/or $C_{12}A_7$), i.e., phases that are mainly responsible for the development of high and early strengths.

Table 2
Chemical analysis (wt.%) of the two types of limestone

	SiO_2	CaO	Al_2O_3	Cr_2O_3	NiO	Fe_2O_3	MgO	LOI
OPM	6.53	47.4	1.09	0.14	0.07	2.72	0.63	41.22
MW	1.71	52.08	0.38	0.11	0.11	4.06	1.44	39.8

LOI, loss on ignition.

Table 3
Low-grade bauxite that used in the experiments (wt.%)

SiO_2	CaO	Al_2O_3	Cr_2O_3	NiO	Fe_2O_3	MgO	LOI
3.15	7.75	49.80	1.21	0.1	24.4	0.09	11.5

LOI, loss on ignition.

During the manufacture of HAC, the SiO_2 content of raw materials is carefully controlled. Excessive SiO_2 (more than ~ 9%) leads to the formation of the very slowly hydrating phases akermanite (C_2MS_2) and/or gehlenite (C_2AS). Less SiO_2 forms belite (C_2S), a phase normally encountered in Portland cements.

Iron oxides are usually present in alumina cements in the range of 1–16%. In the presence of lime and alumina during the heating process, they form tetracalcium aluminoferrite (C_4AF) or the less desirable olivine (C_2F).

Other oxide impurities can affect the mineralogical composition and thus the quality of cement. In HAC with more than 1% of magnesium oxide, Q phase ($C_{20}A_{13}M_3S_3$ or C_6MA_4S) is formed. Q phase has been studied before [6–8] and shows hydraulic properties relative to the other phases found in calcium aluminates [6].

3. Raw materials

The main raw materials that were used for the smelting reduction production of HAC were FeNi-ERF granulated slag, i.e., the basic metallurgical waste from FeNi production, low-grade diasporic bauxite or its by-products from heavy media separation process (float) and limestone.

3.1. ERF slag

The chemical analysis of ERF slag used in the tests is presented in Table 1. X-ray diffraction (XRD) analysis (Philips X-ray powder diffractometer, CuKα radiation) of the slag used in these trials indicated a large amount of glassy material and minor amounts of fayalite (Fe_2SiO_4). The main problem, however, that arises in the utilization of this slag for HAC production is its high SiO_2 content (30–35%). To overcome this, both reduction of the silicon dioxide as well as dilution with other alumina- and calcium-bearing materials were tested, as discussed later.

Table 4
Content (wt.%) of all the raw materials in the mixtures used in the laboratory tests

	1	2	3	4	5	6	7	8	9	10	11	12
Bauxite	55	62	62	40	52	50	35	35	38	36	38	44
OPM	33	30	30	51	41	40	–	–	–	–	–	–
MW	–	–	–	–	–	–	31	42	46	43	46	44
Slag	13	8	8	9	6	10	35	23	16	20	16	12

Table 5
Chemical analysis (wt.%) in the solidified melts in comparison to HAC specifications

	1	2	3	4	5	6	7	8	9	10	11	12	HAC
Al_2O_3	56.79	49.85	50.97	41.74	46.50	42.53	37.53	41.07	34.16	36.29	39.09	49.18	39.0–50.0
CaO	21.84	27.55	38.28	46.81	41.25	48.39	27.98	27.84	38.62	41.03	40.83	36.61	35.0–42.0
SiO_2	15.34	12.36	8.62	8.68	9.17	7.78	15.00	23.35	8.88	10.34	8.85	8.04	4.5–9.0
FeO_x	0.88	5.05	0.00	0.55	1.80	0.25	16.24	3.48	15.92	10.75	6.02	1.33	1.0–16.0
NiO	0.22	0.06	0.04	0.02	0.00	0.02	0.00	0.03	0.00	0.00	0.06	0.06	–
MgO	0.82	0.87	1.20	1.01	0.62	0.67	2.03	3.23	1.92	2.23	3.94	4.43	Less than 1%

3.2. Limestone

Two types of limestone were used: one from the open pit mines (OPM) for laterite exploitation in the vicinity of LARCO's metallurgical plant, and a metallurgical white (MW) limestone. The chemical analyses presented in Table 2 reveal the differences between these two types of limestone, especially in SiO_2 and MgO contents. The OPM limestone has lower MgO content but higher SiO_2 compared to MW. Thus, the decision for the optimum limestone to be used was examined during the laboratory scale trials.

3.3. Low-grade diasporic bauxite

Low-grade diasporic bauxite (Table 3) was obtained from Silver and Baryte Ores Mining. The main phase detected was diaspore (AlO(OH)). Other constituents were boehmite (AlO(OH)) and hematite (Fe_2O_3). Complete extraction of alumina from diasporic bauxite requires stronger caustic solutions, in addition to higher temperatures and pressures. In practice this means that for low-grade bauxite, especially, containing the more difficult to recover diaspore, the production costs are much higher than when only gibbsite ($Al(OH)_3$) is present.

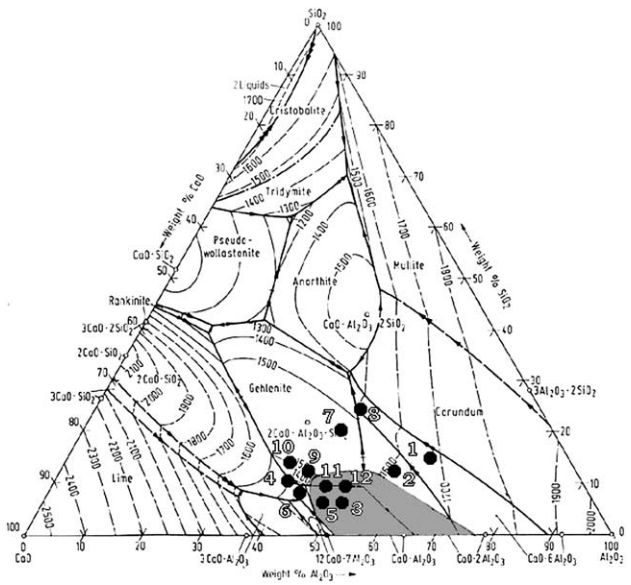

Fig. 1. Laboratory heats in the $CaO–Al_2O_3–SiO_2$ ternary system. Hatched area refers to HAC.

4. Laboratory HAC preparation

The HAC preparation laboratory heat treatments were carried out in a Tammann furnace in graphite crucible. Thermochemical calculations were performed before the heat treatments with ChemSage software [9] after the development of the suitable databases. The calculations showed that the reductions occurring during the heat are strongly enhanced by the parallel use of iron–carbon melt. This metal bath also acts as a collector of the metals produced from the reduction reactions, mainly Ni and Fe.

The set temperature was maintained within an accuracy of ± 20 °C. The furnace was flushed with inert gas to avoid the oxidation of the graphite heating element. The ratios of slag, bauxite and limestone (before calcination) that were used for the heat treatments are presented in Table 4.

Limestone from open pit mines was used in heats 1–6, whereas in heats 7–12 metallurgical white limestone was utilized.

Mixtures of slag, bauxite, limestone and carbon powder were charged in the iron-containing graphite crucible. Slag samples were taken at predetermined time intervals by means of an iron rod in order to measure the kinetics of the reduction reactions.

Three types of cooling processes were tested. In heats 1–10, the cooling rate was ~ 200 °C/h, as the slag was

Table 6
Experimental parameters and results for the mixtures of tests 3, 5, 11 and 12

	3	5	11	12
Limestone used	OPM	OPM	MW	MW
Cooling rate (°C/h)	~ 300	~ 300	~ 100	~ 50
Blaine (cm^2/g)	5250	5250	5250	5250
Compressive strength (MPa) (EN 196-1, w/c = 0.4)				
1 day	–	–	17.4	64.1
7 days	–	–	41.0	80.4
28 days	–	–	54.0	75.9
Main phase(s) detected by XRD	C_2AS	C_2AS	Q and C_2AS	Q and CA

allowed to cool, after heating, in the air within the crucible. In heat 11 the slag was cast in a preheated (~ 1000 °C) iron mould and the approximate cooling rate was estimated at ~ 100 °C/h. The lowest cooling rate was accomplished in Trial 12 (~ 50 °C/h) by manual control of the power supply of the furnace.

4.1. Results and discussion

The main results obtained from the laboratory heat treatments can be summarised as follows:

- FeO_x reduction is enhanced with the presence of carbon-rich iron bath from the beginning of the smelting, which is in accordance with the thermochemical calculations.
- The reduction rate of iron oxides is nearly doubled with a 50 °C increase of the temperature. The iron oxide content of the slag phase is less than 5% after about 1 h of reaction at 1550 °C. FeO_x reduction kinetics will be presented in the future.
- As expected, SiO_2 reduction was very slow, even at elevated temperatures of 1650 °C, with maximum 10% reduction in 5 h.

As the reduction of silicon dioxide is a time-consuming reaction that demands high energy, dilution of silicon dioxide with proper additions of bauxite and limestone is the optimum way to achieve SiO_2 content less than 9% in the final product.

The chemical analysis of the solidified melts after the heat treatments is presented in Table 5. For comparison, the allowable chemical analysis range of the commercial HAC cement is also given. In heats 1–6, the MgO content fulfills the requirement for HAC due to the use of OPM limestone. The final solidified melts from heats 7–12 show an MgO content out of the range for HAC cements when metallurgical limestone with higher MgO content than OPM was used. Iron oxides are within the requirements or lower for all the heats. An almost total recovery of nickel was also achieved, as calculated from the final NiO contents in Table 5.

The Al_2O_3, CaO and SiO_2 contents (%) of the mixtures are plotted in the Al_2O_3–CaO–SiO_2 ternary diagram (Fig. 1) with respect to the HAC area. Four of the final slags (heats 3, 5, 11 and 12) are inside the HAC area. The main experimental parameters and results of the final products of these heats are presented in Table 6.

Table 7
Pilot heat charge (in kilograms)

	1	2	3	4
Cast iron	500	500	500	100
Scrap Fe	1200	1200	1200	1500
Coke	100	20	100	50
Graphite	140	40	200	50
Bauxite	1000	1350	1000	910
Limestone	700	750	700	490
ERF slag	350	300	300	230

Table 8
Final solidified melts in the pilot tests—compositions (wt.%)

	1	2	3	4
Al_2O_3	36.28	40.39	39.42	44.26
CaO	39.72	19.60	35.10	30.20
SiO_2	12.58	3.25	9.67	8.43
MgO	10.50	21.08	12.62	3.08
FeO_x	0.67	3.75	2.54	14.03

The heat treatments presented in Table 6 can be divided into two groups, 3 and 5 with high cooling rate (~200 °C/h) and 11 and 12 with lower cooling rates (100 and 50 °C/h, respectively). The absence of strengths in the final products of the first group can be attributed to the presence of gehlenite, which is the main phase identified with XRD analysis, a phase with no hydraulic activity [10]. The final products of the other group (Trials 11 and 12) developed early strengths, and especially for Trial 12 the final strengths (28 days) are close to those of HAC cements. The main phases identified with XRD were Q phase ($C_{20}A_{13}M_3S_3$) and gehlenite (C_2AS) in Trial 11, and Q phase and CA in Trial 12. Q phase is an MgO analogue of pleochroite in the HACs.

The MgO content of the final products from Trials 11 and 12 was out of the range for HAC (3.9% and 4.5%). The development of strength in test 11 is attributed to the presence of Q phase that was crystallized in the final mixture due to the MgO content and the low cooling rate. The presence of CA in test 12 had a positive effect in the strength development, as indicated in Table 6.

As a general conclusion of the laboratory tests it can be stated that the desirable chemical composition by itself is not adequate to characterize the solidified melt as HAC. The cooling rate of the melt combined with the appropriate mineralogical composition of the product provides the most

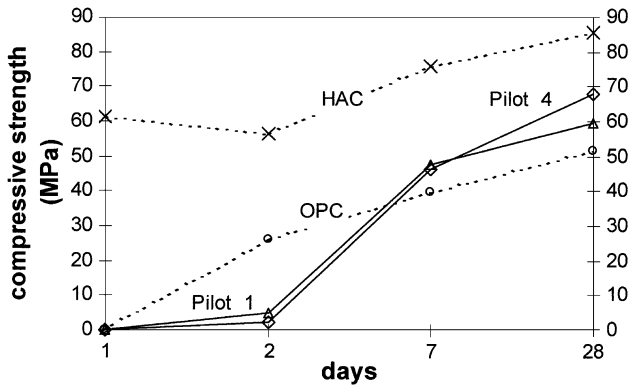

Fig. 2. Compressive strength of pilot product 1 and 4 in comparison with HAC and ordinary Portland cement (w/c ratio = 0.4).

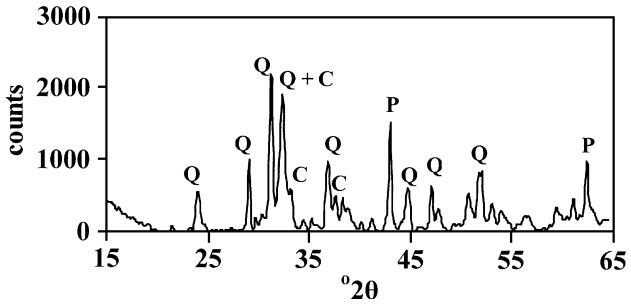

Fig. 3. X-ray diffraction pattern of the pilot product from Trial 1 (Q, Q phase; P, MgO; C, C_2S).

determining factor for the development of compressive strengths.

5. Pilot HAC production

The pilot production tests for HAC were performed in 1.2 MW EAF of Halyvon, Aspropyrgos, Greece. The raw materials used in the pilot heats were cast and scrap iron, coke, graphite, low-grade bauxite, metallurgical white limestone and ERF slag. Four heat treatments were performed, aiming at the production of a final mixture with cementitious properties. The charge calculation was based on the results of the laboratory trials.

Initially the EAF was charged with coarse-grained coke (~ 20 mm), cast iron and iron scrap. After melting of the metal, limestone, bauxite, ERF slag and fine graphite were added. The amounts used are presented in Table 7. Fine graphite was used to accelerate the carbon dissolution in the metal bath and to increase the reduction rate. The melt formed was kept at a temperature from 1500 to 1700 °C for 0.5 to 2 h to achieve the desired degree of reduction of Fe oxides. Then the melt was tapped in a ladle and subsequently cast in 50 × 50 × 50-cm moulds. After a 24-h cooling period, the solidified melt was crushed and subsequently analyzed. The cooling rate was estimated at 120–150 °C/h.

In test heats 1, 2 and 3, magnesite bricks constituted the lining of the EAF. Considerable lining wear was observed, reflected also in the high MgO content of the melt produced. With the use of magnesite–chromite bricks (heat 4) the lining wear was drastically reduced.

5.1. Results and discussion

In Table 8 the analyses of the pilot heat treatments products are given. All the final products are within the allowable range of HAC analysis with respect to Al_2O_3 and FeO_x contents. CaO is acceptable for Trials 1, 3 and 4, and SiO_2 is within or close to the HAC specifications (up to 9%), apart from Trial 1. The high MgO content observed in heats 1 to 3 is due to magnesite brick wear as the formed melt attacks the basic lining severely. By the use of magnesite–chrome lining, this problem was eliminated and 3.08% of MgO was measured in the final melt.

Due to its high SiO_2 content, the amount of ERF slag charged was limited from 12% to 17% of the total raw material weight. The lowest silica content was observed in Trial 2 (3.25%) with 12% slag, but CaO and MgO showed a divergence from the HAC specifications. The best results were achieved in Trial 4, where all the major oxides including silica (8.43%) were within the range of HAC. Slag utilization in this case was 14%.

The recovery of nickel from the ERF slag and bauxite is important for the economics of this process. Nickel in ERF slag is in the form of metallic losses (entrapped FeNi grains) or chemically bonded Ni^{2+} [11]. According to the mass balances, Ni recovery was 87% on average for the four pilot heat treatments.

High reduction of the Fe oxides was achieved in heats 1 to 3. In Trial 4, only a partial reduction of iron oxides down to 15% was achieved by appropriate deduction of the heat treatment duration.

The final products were ground to four different predefined finenesses, 4050, 4300, 5300 and 6800 cm^2/g, by means of a pilot 5-kg ball mill. All samples were prepared according to EN 196-1. Higher compressive strengths were achieved in the products of pilot tests 1 and 4: 60 and 68 MPa for 28 days and 5300 cm^2/g, respectively. In Fig. 2, the development of the strengths is presented together with the HAC and OPC cements. It is observed that the products of tests 1 and 4 show 4.7 and 2 MPa early strengths in 2 days, compared to 26.2 and 56.6 MPa of OPC and HAC, respectively. However, in 7 days they developed strengths of 47.5 and 46.5 MPa, higher than the 39.7 MPa of OPC but lower than the 76.1 MPa of HAC. The same trend is also found in the 28-day strengths with 59.6, 68.0, 51.5 and 81.4 MPa for the products of heats 1 and 4, OPC and HAC, respectively.

Representative XRD patterns of the solidified melts of heats 1 and 4 are presented in Figs. 3 and 4. The differences in the chemical compositions of these melts to products are also reflected in the XRD patterns. In heat 1 (Fig. 3) the peaks of Q phase, C_2S and periclase are prevailing. In heat 4 (Fig. 4) the high amount of Fe oxides led to the crystallization of wustite, apart from Q phase and C_2S.

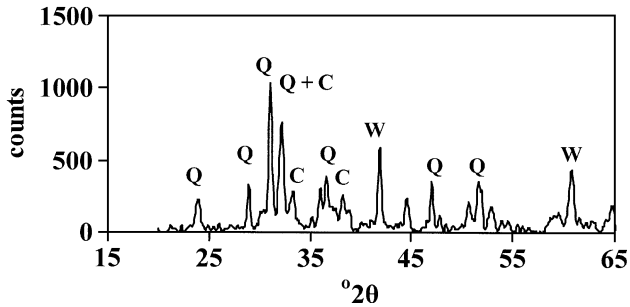

Fig. 4. X-ray diffraction pattern of the pilot product from Trial 4 (Q, Q phase; W, FeO; C, C_2S).

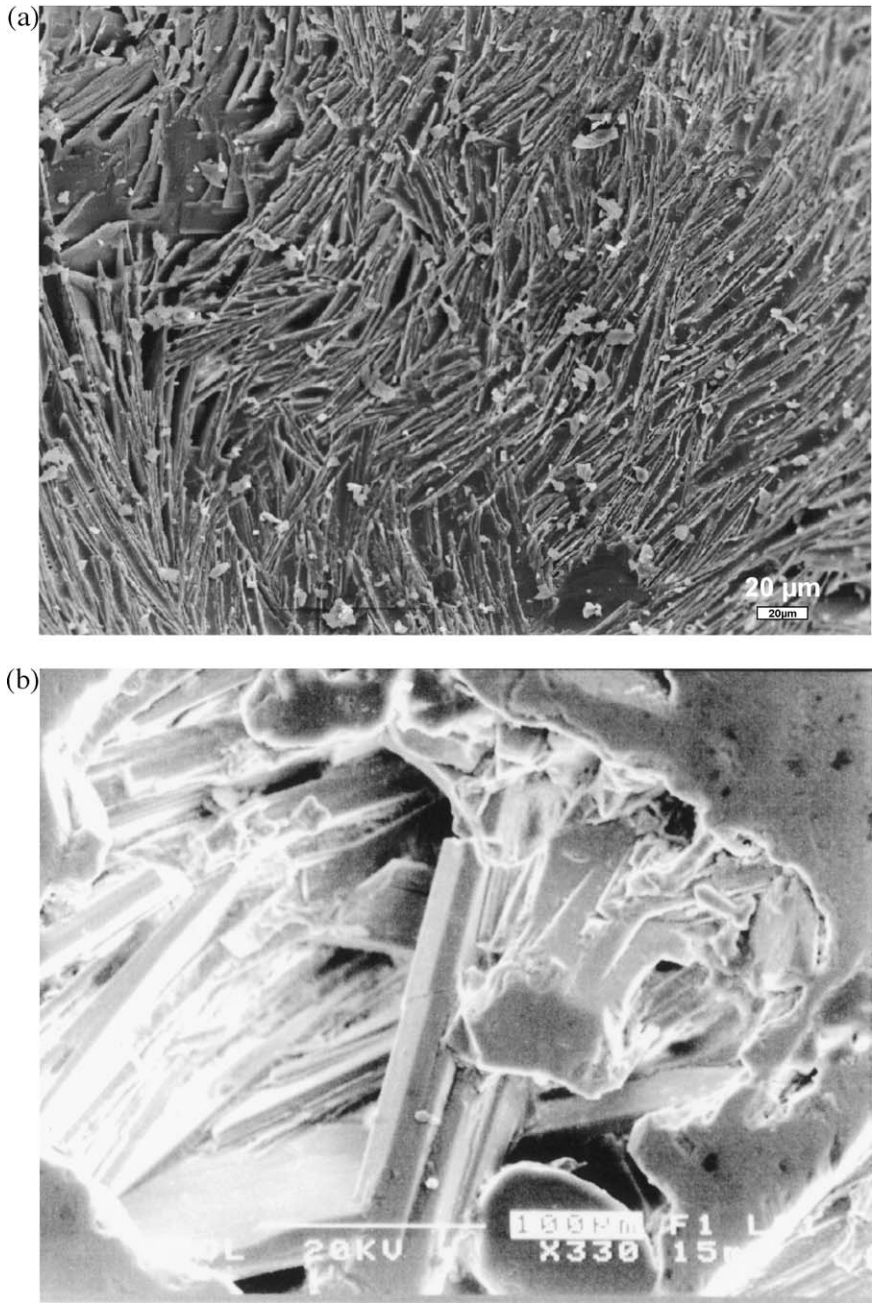

Fig. 5. Q phase crystals pilot product 1 (a) and laboratory trial 12 (b) (magnification, × 330).

SEM observation of the facets of fractured segments of the solidified melts from heat 1 revealed associations of elongated, fibrous, prismatic Q-phase crystals. In Fig. 5(a) and (b) the Q-phase crystals formed in pilot heat 1 and laboratory heat 12, respectively, are depicted. In the latter case, the crystals are enlarged in comparison to the former ones. This is attributed to the higher cooling rate that existed in the pilot heats with respect to the laboratory heat 12 (120–150 and 50 °C/h, respectively).

Energy dispersive spectroscopy microanalyses of the Q phase formed in pilot test 1 and laboratory test 12 are presented in Table 9. These results are in agreement with the $CaO–Al_2O_3–SiO_2$ (with 5% MgO) phase equilibrium diagram (Fig. 6) [12].

Table 9
Mean chemical analysis (wt.%) of the Q crystals in pilot test 1 and laboratory test 12

	Pilot heat 1	Laboratory heat 12
CaO	50.0	56.0
Al_2O_3	34.0	35.0
SiO_2	11.2	4.9
MgO	4.4	3.8

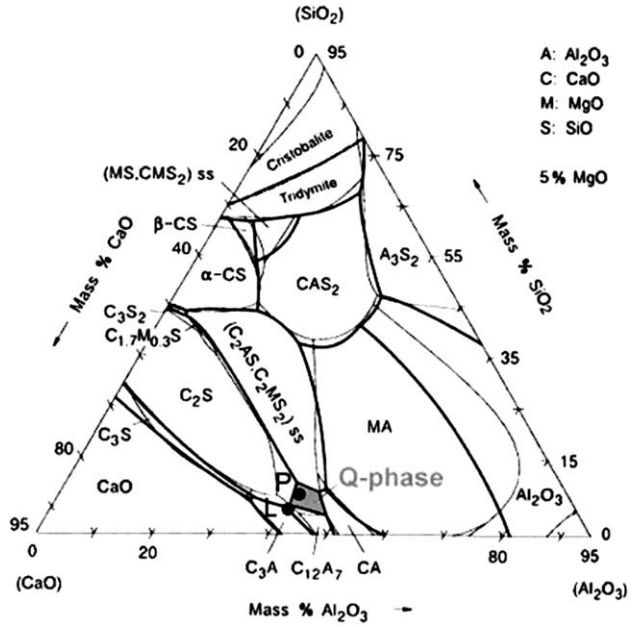

Fig. 6. $CaO-Al_2O_3-SiO_2$ with 5% MgO ternary system. Hatched area refers to Q phase. P, pilot test 1; L, laboratory test 12.

Bearing in mind the complexity of the hydration mechanisms in heterogeneous systems such as these products, there is no definite explanation about the low early strengths of the pilot products. The hydration mechanism is still being investigated.

6. Conclusions

The production of HAC by reduction smelting of FeNi-ERF slag mixtures with low-grade diasporic bauxite and limestone is feasible. The products of laboratory tests smelted in graphite crucibles developed compressive strengths and are within the allowable range of the chemical analysis of the HAC.

Pilot-scale tests in 1.2 MW EAF gave products with high MgO content due to magnesite brick wear from the acid slag formed. Replacement with a magnesite–chrome lining eliminated this problem and resulted in a product with 3.08% MgO, similar to that of laboratory tests. These products developed low early compressive strengths. However, the 7- and 28-day strengths were higher than those of OPC.

Concerning the main process parameters, SiO_2 reduction was time-consuming and demanded high energy. The presence of an underlying carbon-rich metal bath enhanced the reduction rate. The recovery of Ni contained in ERF slag and bauxite was almost quantitative in the laboratory tests and averaged 87% in the pilot tests.

The reduction smelting process of the ERF slag with limestone and low-grade diasporic bauxite shows a considerable potential for optimization. The process proposed in this study is environmentally acceptable and can prove to be economically beneficial since it is based on the recycling of metallurgical residues and the use of low-cost raw materials.

Acknowledgements

The authors gratefully acknowledge the financial support provided by the General Secretariat for Research and Technology as this work was performed in the frame of the second Operational Programme for Research and Technology (E.P.E.T. II) sponsored research project (contract No. EKBAN #385).

Moreover, the authors thank G. Danassis, Halyvon, for his contribution.

References

[1] J.E. Kopanda, G. Maczura, Production processes, properties and applications for calcium aluminate cements, in: L.D. Hart (Ed.), Alumina Chemical Science and Technology Handbook, American Ceramic Society, Westerville, OH, 1990, pp. 171–184.
[2] C.M. George, Manufacture and performance of aluminous cement: a new perspective, in: R.J. Mangabhai (Ed.), Calcium Aluminate Cements, Spon, London, UK, 1990.
[3] K.L. Scrivener, J.L. Cabiron, R. Letourneuxet, High-performance concretes from calcium aluminate cements, Cem. Concr. Res. 29 (1999) 1215–1223.
[4] B. Stivanakis, E. Galanoulis, D.C. Papamantellos, Contribution to the utilization of flying ash in the cement industry, Technika Chronika. Scientific Journal of the T.C.G., Section C 2 (1–2) (1982).
[5] P. Nikolopoulos, D.C. Papamantellos, B. Stivanakis, Utilization Megalopolis flying ash in the cement industry, "Utilization of Greek Flying Ash" Symposium, Technical Chamber of Greece, Athens, Greece, 29-11-88.
[6] I. Kapralik, L. Stevula, F. Hanic, Hydration and hydraulic properties of the Q-phase in the system $CaO-Al_2O_3-SiO_2-MgO-H_2O$ referred to high-alumina cement, Cem. Concr. Res. 19 (1989) 519–526.
[7] I. Kapralik, F. Hanic, Studies of the System $CaO-Al_2O_3-MgO-SiO_2$ in relation to the quaternary phase Q, Trans. J. Br. Ceram. Soc. 79 (1980) 128–133.
[8] F. Hanic, M. Handlovic, I. Kapralik, The structure of a quaternary phase $Ca_2OAl_{32-2v}Mg_vSi_vO_{68}$, Acta Crystallogr., B 36 (1980) 2863–2869.
[9] G. Eriksson, K. Hack, Chemsage—a computer program for the calculation of complex chemical equilibria, Metall. Trans., B, Process. Metall. 21 (1990) 1013–1023.
[10] F.M. Lea, The Chemistry of Cement and Concrete, Edward Arnold, London, 1970.
[11] A.S. Diamantopoulos, G.N. Angelopoulos, D.C. Papamantellos, Investigation of the sedimentation of FeNi fine grains entrained in ERF slag, Steel Res. 67 (1996) 179–187.
[12] M. Allibert, et al., Slag Atlas, 2nd ed., "Phase diagrams", Verlag Stahleisen, Dusseldorf, 1995, p. 160 (Edited by VDEh).